BNL-105207-2014-TECH

Booster Technical Note No. 163;BNL-105207-2014-IR

BOOSTER DIPOLE MAGNET HALF-CELL ALIGNMENT INCLUDING MAGNET FRINGE FIELD EFFECTS

M. A. Goldman

April 1990

Collider Accelerator Department

Brookhaven National Laboratory

U.S. Department of Energy

USDOE Office of Science (SC)

DISCLAIMER

BOOSTER DIPOLE MAGNET HALF-CELL ALIGNMENT

INCLUDING MAGNET FRINGE FIELD EFFECTS

BOOSTER TECHNICAL NOTE
NO. 163

M. A. GOLDMAN

APRIL 16, 1990

ALTERNATING GRADIENT SYNCHROTRON DEPARTMENT
BROOKHAVEN NATIONAL LABORATORY
UPTON, NEW YORK 11973

BOOSTER DIPOLE MAGNET HALF-CELL ALIGNMENT

INCLUDING MAGNET FRINGE FIELD EFFECTS

M.A. Goldman
February 22, 1989

Introduction

This note discusses alignment of the Booster dipole magnets with respect to the quadrupole magnet located on the same half-cell. A good initial alignment is desired because the dipole and quadrupole will be rigidly pinned to the strongback girder on which they stand. After the initial alignment they will not be moveable with respect to one another.

The method of alignment to be used is to establish a visual optical boresight parallel to the quadrupole magnetic axis, and place optical targets at the ends of the dipole magnet pole faces and within the dipole aperture, located so that the dipole magnet will be positioned properly when the centers of these targets both lie on the visual boresight line. The pre-placement of the target centers in the end face apertures is established by prior computational analysis.

In our analysis we make use of particle orbit computations described in [1]: "Deflecting Magnets" by H.A.Enge, appearing in "Focusing Of Charged Particles, Volume 2", A. Septier editor, Academic Press, New York, 1967, and in the paper [2]: "Effect of Extended Fringing Fields on Ion-Focusing Properties of Deflecting Magnets," Rev. Sci. Instr. 35, 278 (1964).

Calculations of the positions of the dipole optical targets are made using Enge's particle-optical results, which include the effects of magnet fringe fields. The calculations are made for the boundary conditions that the particle bending angle is 10 degrees and the particle path length through the dipole magnet is 2.40 meter. (A dipole bending magnet with sharp field cutoff at the pole face boundary edges would have a constant bending radius of 13.75099 meter to achieve 10 degree deflection with 2.40 meter curved path length.) Enge's analysis allows one to compute the target displacement required for proper alignment, when account is taken of the shape and variation of the magnetic fringe field beyond the magnetic pole face boundary edges.

Before calculating the locations of the dipole magnet survey reference markers with respect to the quadrupole magnetic axis, we will review the assumptions made in computing the dipole survey marker positions tabulated in BNL Booster Technical Note No. 119, [3], and in choosing the physical design length selected for the dipole magnets. We will calculate the optical target displacements which would be appropriate under these assumptions. We will subsequently calculate the target displacements which are appropriate when the more extended analysis of Enge is used.

It will turn out that the effect of the extended fringe magnetic field is to move each of the dipole survey markers by an offset of 7 milli-inches, perpendicular to the line segment joining them (directed towards the inside of the particle orbit) when compared to the positions listed in Technical Note No. 119. This implies that the coordinates of the dipole survey markers tabulated in Booster Technical Note 119 should be adjusted to incorporate these displacements, because these tables provide the listing of coordinates which controls the installation of the Booster ring magnets. This can be accomplished by using a commercial surveying program (SURVEYOR 1, Carlson Software, Maysville, Kentucky 41056) and will appear in a future Booster Technical Note.

The General Method Of Alignment

Three spatial reference lines are used to describe the ion optics and geometry of the quadrupole magnet. These are: (1) the geometric axis of symmetry of the magnet, (2) the magnetic axis of the quadrupole, which is the ion-optical axis of the quadrupole, and (3) the survey target axis defined by the centers of the visual optical targets which are placed into the survey bushings above the quadrupole. The magnetic axis can be determined by rotating pickup coil measurements, and thereby located spatially with respect to the geometric symmetry axis. Ideally the geometric symmetry axis and the magnetic axis coincide while the survey axis is parallel to the symmetry axis, and the magnet is oriented so that the survey and symmetry axes define a vertical plane and all three axes are horizontal.

The first step in alignment of the Booster half-cell is to visually define the magnetic axis of the quadrupole magnet so that it determines an optical boresight line which is accessible to autocollimation. To do this, a quadrupole alignment fixture is fabricated (Figure 1). The fixture contains a centered optical target. The fixture can slide along the pole tips of the magnet; the target center motion generates the axis of symmetry of the quadrupole.

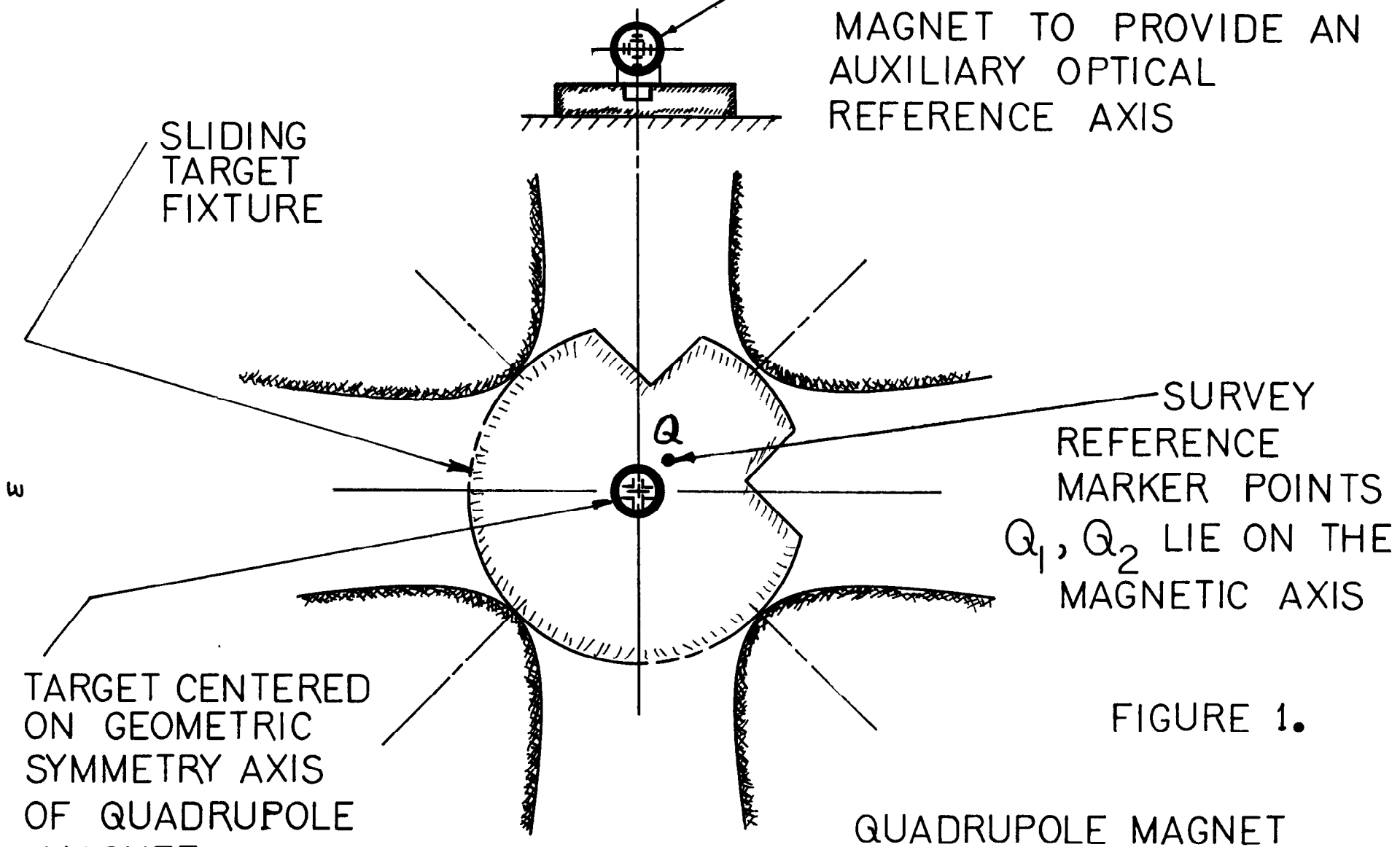
SURVEYOR'S TARGETS LOCATED IN BUSHINGS ABOVE MAGNET TO PROVIDE AN AUXILIARY OPTICAL REFERENCE AXIS
SLIDING TARGET FIXTURE
Q
SURVEY REFERENCE MARKER POINTS Q_1, Q_2 LIE ON THE MAGNETIC AXIS
TARGET CENTERED ON GEOMETRIC SYMMETRY AXIS OF QUADRUPOLE MAGNET
QUADRUPOLE MAGNET REFERENCE AXES

FIGURE 1.

The offset of the quadrupole magnetic axis from the symmetry axis is known, from the rotating coil measurements. The geometric axis is used as the reference visual boresight axis, because the optical targets can be well centered on it. The location of the (parallel) magnetic axis is thereby well defined, because the offset of these two axes has been determined by the coil measurements.

The position of the dipole magnet is determined when the locations of the its face aperture centers are defined and the tilt of the plane pole faces is known. After the magnet has been levelled, the locations of the aperture centers fix the magnet's position. To align the dipole magnet with respect to the quadrupole magnet one proceeds as follows:

One moves the magnetic axis of the quadrupole magnet into proper position with respect to the dipole survey markers. To accomplish this one inserts an optical target fixture into each end face of the dipole magnet. The fixtures are designed so that their target centers are colinear with the visual boresight axis defined by the geometric symmetry axis of the quadrupole magnet, when the quadrupole and dipole magnets are in proper alignment with respect to one another.

The target displacements from quadrupole geometric boresight must be obtained by calculation, from a knowledge of the trajectories of the particles traversing the magnets.

At the top of the dipole magnets are survey bushings, which accept optical alignment targets. The target centers can provide alternative reference points for the dipoles. The positions of these target centers are measured with respect to the end face center points, so that accessible geometric reference points can be provided when the magnet aperture is no longer physically or visually accessible to optical survey instruments.

Calculation Of The Dipole Magnet Alignment Target Offsets

(In the calculations to follow, the chordal distance between the center points D1 , D2 of the dipole end face apertures is assumed to be 2.3147 meter, which is the chordal distance between the dipole magnet survey markers reported in [3]. The bending radius of the closed orbit particle trajectory within the pole faces is assumed to be 13.75099 meter, as specified on page 1-10 of the Booster Design Manual [6] .

The calculation of the target center positions is presented in the pages to follow. The distances to be calculated are the horizontal displacements of the target centers, from the centers of the end face apertures.

It will turn out that the dipole target center horizontal offsets from the end face aperture centers are: 10 milli-inches outwards of aperture center for the target proximal to the quadrupole magnet, and 8.071 inch outwards of center for the target distal to the quadrupole magnet. Each offset is measured in the lamination end plane defining an edge of the pole face boundary.

The Alignment Geometry

We define the following points, lying in the horizontal midplane of the dipole. We assume that the dipole magnet has already been levelled and the magnetic axis of the quadrupole magnet lies in this plane. Referring to Figure 6, let:

T_m be the closed orbit center of curvature,

D1 be the symmetry center of the dipole magnet's end face (pole boundary face) proximal to the quadrupole magnet,

D2 be the symmetry center of the dipole magnet's end face distal to the quadrupole magnet,

Q1, Q2 be survey marker points on the quadrupole magnet's magnetic axis,

P1 be the intersection point of the quadrupole magnet's optical axis with the proximal pole face boundary plane,

P2 be the point of intersection of the quadrupole magnet's optical axis with the distal pole face boundary plane.

We define the following geometric objects, in accord with Enge:

VFB and VFB' are the virtual field boundary planes which are parallel to the pole face boundaries at the dipole magnet ends, for the Sharp Cutoff Fringing Field calculation,

s is the distance between each dipole pole face and its neighboring virtual field boundary plane, measured in units of the dipole magnet gap length,

g is the dipole magnet gap (in Enge's papers the symbol D is used),

S1 and S2 are intersection points of the circle, $\mathcal{C}$, having center at T_m and also passing through D1 and D2, with the planes VFB and VFB' respectively,

NVFB and NVFB' are lines perpendicular to the virtual field boundary planes at points S1 and S2 respectively.

SCOFF and SCOFF' are central reference rays for the optical calculation, as defined by Enge [1,2]. They are rays parallel to the particle's asymptotic entry and exit trajectories and pass through S1 and S2, respectively.

EFF and EFF' are the asymptotic closed orbit trajectory rays (parallel to rays SCOFF and SCOFF' respectively), defined by Enge for the extended fringing field (EFF) approximation, before entry to and exit from the extended magnet fringing fields,

We let:

θ_p be the angle between the dipole magnet end pole faces; this is the physical dihedral wedge angle of the magnet, as specified in the design drawings (9.6560 degrees),

θ_m be the orbit deflection angle , exactly 10 degrees,

μ be the angle $\theta_m/2 - \theta_p/2$,

α be the angle between NVFB and EFF,

β be the angle between NVFB' and EFF',

Δ Y1 be the distance between the parallel rays EFF and SCOFF,

Δ Y2 be the distance between the parallel rays EFF' and SCOFF',

ρ_g be the geometric radius of the dipole magnet, that is the distance from aperture center points D1,D2 to the line of intersection of the end face planes (Fig. 2),

ρ_m be the bending radius of the closed orbit particle trajectory deep interior to to the pole face boundary,

$\psi/2$ be the angle S1-T-D1 .

The calculation of the alignment target locations to be used during alignment of the half cells proceeds as follows:

We wish to calculate the optical target center displacements $|\overline{D1\text{-}P1}|$ and $|\overline{D2\text{-}P2}|$, along the pole faces, which give correct target placement to allow magnet alignment on the support girder of the half cell.

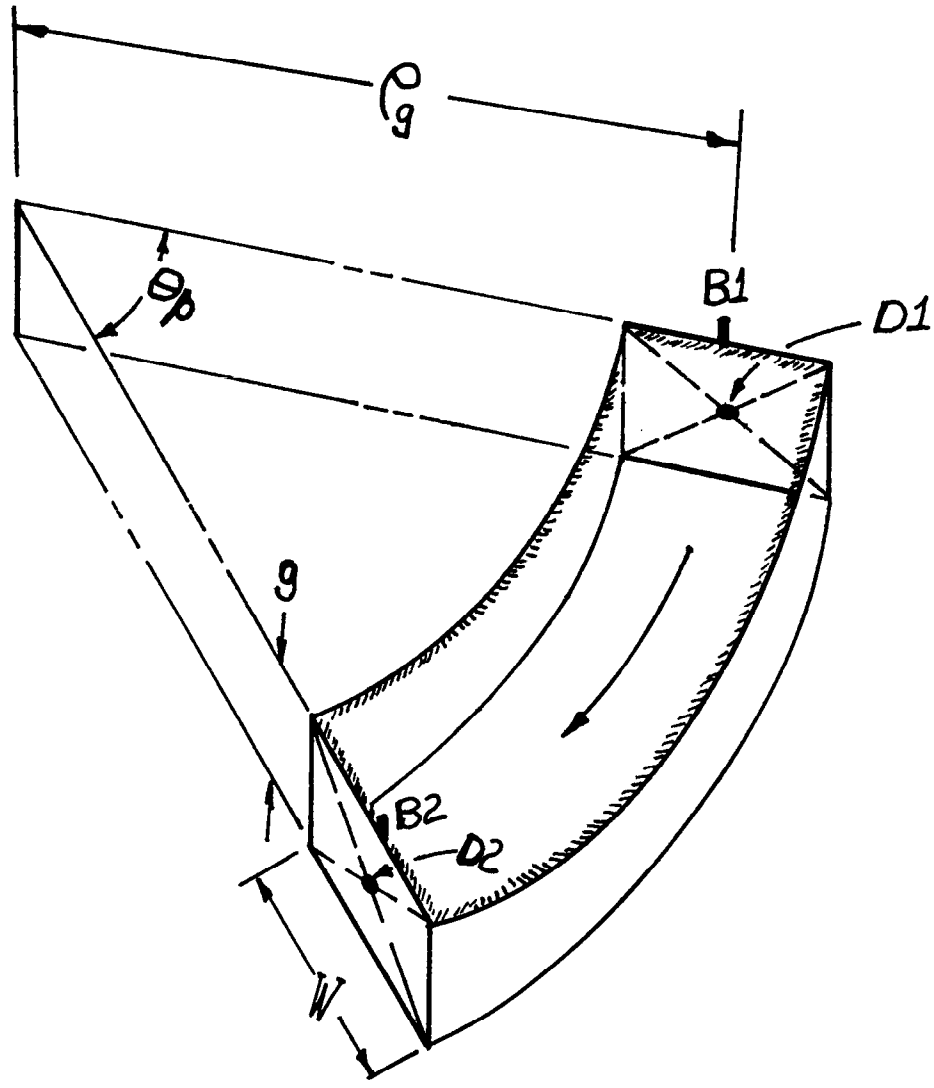

$g = 3.25''$

$W = 10.0''$

$\theta_p = 9.656°$

$\rho_g = 541.380''$

SURVEY REFERENCE MARKER POINTS D1, D2 ARE AT LAMINATION END SURFACE APERTURE CENTERS

FIGURE 2. THE DIPOLE MAGNET

We will first calculate the target center displacements using the assumptions of G.F. Dell, in reference [3]. Here, the parallelism of the virtual field boundaries to the dipole magnet end faces is not retained, and the distance between the assumed virtual field boundaries for sharp fringing field cutoff is assumed to be one half of the magnet pole spacing, measured along a circular arc of bending radius ρ_m . In this approximation the entry trajectory of the reference particle is assumed to lie on the quadrupole's magnetic optic axis, up to the point of intersection, M1, of the optic axis with the sharp cutoff virtual field boundary (Fig. 3). The particle then travels on a circular trajectory of radius ρ_m until it leaves the magnetic field (which has an abrupt cutoff) at point M2 and exits along a straight ray directed 10 degrees to the entry ray. The entry and exit rays are assumed to be tangent to the circular trajectory arc. The two dipole magnet survey marker points, D1 and D2 , are assumed to lie on the curved particle trajectory. The wedge shaped regions of constant fringing field are assumed to extend beyond the laminations at each end of the dipole magnet by a distance g/2 , measured along the arcs M1-D1 and M2-D2 . To achieve this the dipole magnet wedge angle is chosen according to the criterion: $(\theta_m - \theta_p)\,\rho_m = g$. This gives $\theta_p = 9.6560$ degrees. The dipole magnet wedge angle has, in fact, been designed to be this angle. The relevant geometry is illustrated in Fig. 3 . By simple trigonometry, one gets target offset lengths $|\overline{P1\text{-}D1}| = 0.0024"$ and $|\overline{P2\text{-}D2}| = 8.0633"$ under these assumptions.

We now use particle trajectory calculations by H.A. Enge (described in references [1],[2]), in order to take into account the effects of a finite gradient of fringing field.

Enge locates the asymptotic entrance ray EFF of the particle trajectory (with extended fringing field), and the corresponding exit ray EFF', by computing their lateral displacements $\Delta Y1$ and $\Delta Y2$ from parallel rays SCOFF and SCOFF' respectively. The rays SCOFF and SCOFF' are determined on the basis of a sharp cutoff fringing field approximation where particles are bent with constant curvature in a constant magnetic field which terminates abruptly on "virtual field boundary" surfaces. The sharp cutoff fringing field approximation assumes that the rays SCOFF, SCOFF' are each tangent to a circle of radius ρ_m , the magnetic bending radius well interior to the pole face boundary. This circle passes through the dipole magnet aperture centers D1,D2 . The rays terminate, meeting the bending circle as tangents at points S1,S2, where they intersect the "virtual field boundary" planes VFB and VFB' which are parallel to the magnet end faces.

$$\lambda \equiv \frac{\theta_m}{2} + \frac{\theta_p}{2} = 9.828°$$

$$\mu \equiv \frac{\theta_m}{2} - \frac{\theta_p}{2} = 0.1720°$$

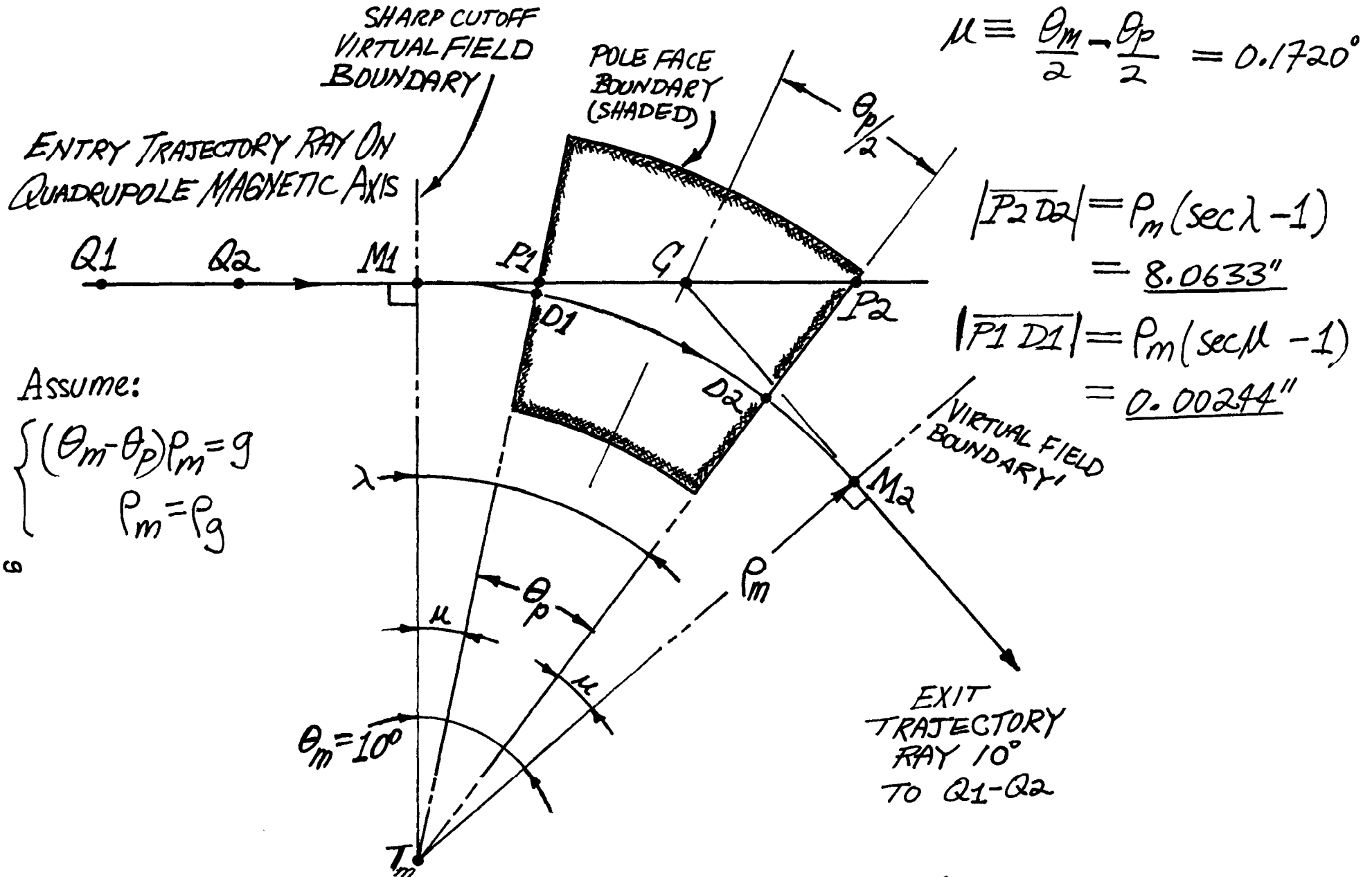

$$|\overline{P_2 D_2}| = \rho_m(\sec\lambda - 1) = \underline{8.0633"}$$

$$|\overline{P_1 D_1}| = \rho_m(\sec\mu - 1) = \underline{0.00244"}$$

Assume:

$$\begin{cases} (\theta_m - \theta_p)\rho_m = g \\ \rho_m = \rho_g \end{cases}$$

FIGURE 3. HALF-CELL ALIGNMENT BASED ON ASSUMPTIONS OF BOOSTER TECHNICAL NOTE No. 119.

The spacing of each virtual field boundary plane to its parallel end pole face has been calculated by Enge. Enge computes two cases, corresponding to the particular nature of the magnetic field falloff profile at the pole end face. These are for "short-tail" and "long-tail" fall profiles, which correspond to different magnet aperture gap height-to-width aspect ratios. The distance between the virtual field boundary plane and the end pole face plane is $sg = 0.62g$ for the short-tail case and $sg = 0.68g$ for the long-tail case, where g is the gap width. According to G.F. Dell ([4],[5]) the short-tail case, with $s = 0.62$, corresponds to the Booster dipole magnet design. Equations (74) through (76) of Enge's article give the displacements $\Delta Y1$, $\Delta Y2$ of ray EFF from SCOFF and EFF' from SCOFF' in terms of the angles α , between SCOFF and the normal to VFB , and β , between SCOFF' and the normal to VFB' , and also the the value of the integral I1 in (75); for the short-tail case $I1 = 0.309$.

First order ray optical calculations have been carried out using ray transfer matrices appearing in [2]. These calculations were performed assuming that it was possible to achieve proper particle trajectories without changing the particle bending radius from the value ρ_m specified in the Booster Design Manual. It was not, in fact, possible to achieve symmetric entry and exit trajectories with respect to the dipole magnet and also have small offsets of these trajectory rays from the design values and, at the same time have the correct bend angle. The cause of this situation is the presence of an extra 0.12 gap length of fringing field at each end of the magnet, above the length 0.50g assumed when the magnet was designed. The optical calculations for this case are somewhat complicated, and appear in Appendix 2.

The relevant geometry is shown in Fig. 6. The particle entry and exit rays are not parallel to the rays SCOFF , SCOFF' (defined by Enge) because the magnet wedge angle is, by design, 9.656 degrees (selected according to the criterion of [3]) rather than 10 degrees = ρ_m which would be desired according to the more detailed analysis by Enge [2]. Optical ray transfer cofficients are given in reference [2] which allow a first order ray-optical matrix calculation of the entry and exit ray positions and, thereby, the dipole survey point positions. The ray transfer matrix elements used are the modified elements needed for the extended fringe field computations.

The calculation gives target offsets $|\overline{P1-D1}| = -0.772"$ and $|\overline{P2-D2}| = 7.289"$. These offsets are much larger in magnitude than the offsets calculated previously for the conditions of [3]. This is not accidental. The analysis of Enge points out that the

fringing fields extend effectively 0.62 gap widths beyond each pole face, not 0.5 gap widths. This gives an increase of bending region 2 x 0.12 x 3.25" = 0.780" in length as compared with the previous calculations, and this extra length of bending region is compensated for by changed entry and exit ray offsets. The error caused by non-parallelism of the pole ends to the virtual field boundaries, in [3], causes small error.

The large entry and exit ray offsets needed to operate with the same particle bending radius are unacceptable, because of the larger aperture required for the particle beam. Fortunately, it will turn out that one can select a bending radius which will allow the correct particle bending angle, with equal entry and exit ray displacements from SCOFF, and with small change of trajectory length (0.002") of the 2.40 meter trajectory; at the same time the lateral displacement of the dipole survey marker line D1-D2 from the position required in Booster Technical Note No. 119 is small (0.007").

The relevant geometry for the ray optics with modified bending radius is shown in Fig.4A. By increasing the particle bending radius appropriately, it is possible to have the reference ray SCOFF tangent to the circular arc through the points S1, D1, D2, S2 and have the ray SCOFF' (which is also tangent to this arc) deviate by the desired 10 degree bending angle from SCOFF. In this case the particle entry ray Q1-Q2 (along the quadrupole magnetic axis) can be coincident with the ray EFF. The particle exit ray is then along EFF'. The entry and exit ray deviations from the sharp cutoff reference rays are then minimal, the deviations are equal at entry and exit from the dipole, the dipole is located symmetrically with respect to the entrance and exit trajectories, and the correct trajectory deviation angle is achieved.

The computation of the modified bending radius and target offsets appears in Fig. 4B and the pages following. The offset of the proximal target from the center of the dipole end face is 0.010". The offset of the distal target from the center of the dipole end face is 8.071". The new bending radius is 545.837". The calculation given in Fig. 5 indicates that the total path length of trajectory changes little (about -0.002") when the new bending radius is used.

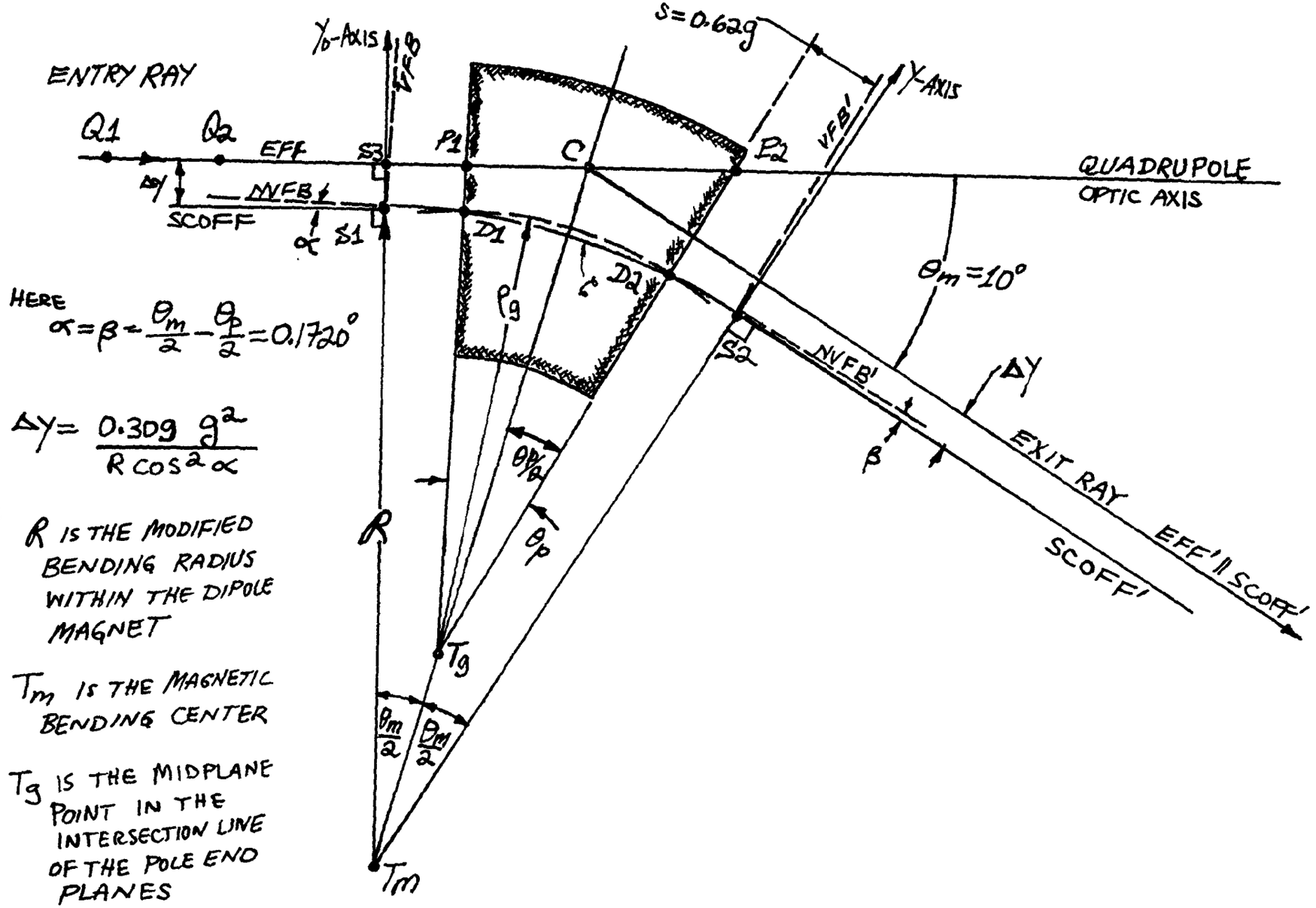

R IS THE MODIFIED BENDING RADIUS WITHIN THE DIPOLE MAGNET

T_m IS THE MAGNETIC BENDING CENTER

T_g IS THE MIDPLANE POINT IN THE INTERSECTION LINE OF THE POLE END PLANES

FIGURE 4A. GEOMETRY FOR MINIMAL TARGET OFFSET, ASSUMING EXTENDED FRINGING FIELD SHORT-TAIL DISTRIBUTION AND MODIFIED BENDING RADIUS.

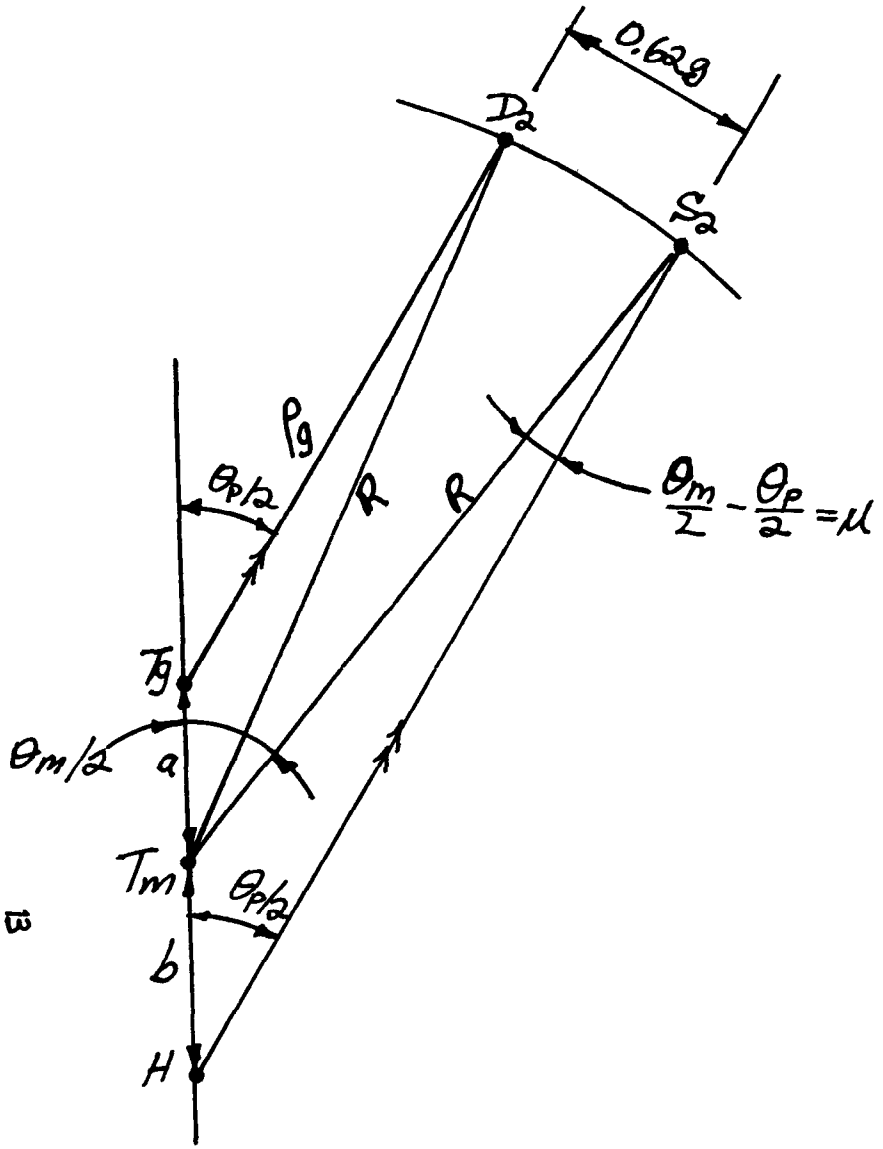

DRAW A LINE THROUGH S_2 PARALLEL TO THE POLE EDGE $T_g D_2$. CALL H ITS POINT OF INTERSECTION WITH THE LINE OF CENTERS $T_m T_g$.

CALL $|T_g T_m| = a$, $|T_m H| = b$.

SINCE S_2 IS AT A DISTANCE $S_g = 0.62g$ FROM $D_2 T_g$ WE HAVE:

$$|T_g H| = a+b = \frac{0.62g}{\sin\left(\frac{\theta_p}{2}\right)} = \frac{S_g}{\sin\left(\frac{\theta_p}{2}\right)}.$$

APPLY THE LAW OF SINES TO $\Delta H T_m S_2$:

$$b = R\left[\frac{\sin\mu}{\sin\left(\frac{\theta_p}{2}\right)}\right].$$

THIS GIVES:

$$a = \frac{S_g}{\sin\left(\frac{\theta_p}{2}\right)} - R\left[\frac{\sin\mu}{\sin\left(\frac{\theta_p}{2}\right)}\right].$$

APPLY THE LAW OF COSINES TO $\Delta T_g T_m D_2$:

$$(a/P_g)^2 + 1 + \left(\frac{2a}{P_g}\right)\left(\cos\frac{\theta_p}{2}\right) = (R/P_g)^2.$$

SET $U = \dfrac{(S_g/P_g)}{\sin(\theta_p/2)} = \dfrac{0.62 \times 3.25''/541.38''}{\sin(9.6560°/2)} = 0.044223$

$V = \left(\dfrac{\sin\mu}{\sin\theta_p/2}\right) = \dfrac{\sin(0.172°)}{\sin(9.6560°/2)} = 0.035\,6676$

$\xi = R/P_g$, AND SOLVE EQUATIONS ABOVE FOR ξ!

FIGURE 4-B. CALCULATION OF MODIFIED BENDING RADIUS R FOR MINIMUM OFFSET TARGET GEOMETRY.

ONE GETS: $a/\rho_g = u - \xi v$ AND $(u-\xi v)^2 + 1 + 2(u-\xi v)\cos\theta_p/2 = \xi^2$.

THE QUADRATIC EQUATION IS SOLVABLE FOR ξ. WRITING

$A\xi^2 + B\xi + C = 0$ WHERE $A = 1 - v^2 = 0.9987278$

$B = (2v)(u + \cos\theta_p/2) = 0.0742366$

$C = (-1)(1 + u^2 + 2u\cos\theta_p/2) = -1.0900864$ ONE GETS

$\xi = R/\rho_g = \underline{\underline{1.0082323}}$ AND ALSO THE DISTANCE BETWEEN CENTERS

$|\overline{T_g T_m}| = a = \rho_g(u - \xi v) = \underline{4.47243''}$.

$R = (1.0082323)\rho_g = (1.0082323)(541.380'')$

$\underline{R = 541.38'' + 4.457'' = 545.837''}$

WE NOW FIND THE OFFSET, ΔY, BETWEEN RAYS SCDFF, EFF BY USING EQUATION (76) OF REFERENCE [2]:

$\Delta Y = g^2 I_1 / R\cos^2\alpha$ WHERE $I_1 = 0.309$ FOR THE SHORT-TAIL FRINGE FIELD DISTRIBUTION,

$g = 3.250''$ AND, HERE,

$\alpha = \theta_m/2 - \theta_p/2 = 0.1720''$.

IN TRIANGLE $T_m C S_3$ OF FIGURE 4A WE HAVE: $|\overline{T_m C}| = (R + \Delta Y)\sec\frac{\theta_m}{2} = \underline{547.92781''}$,

GIVING $|\overline{T_g C}| = |\overline{T_m C}| - |\overline{T_g T_m}| = \underline{543.45538''}$.

WE THEN GET THE TARGET CENTER OFFSETS $|\overline{D_2 P_2}|$ AND $|\overline{D_1 P_1}|$ BY APPLYING THE LAW OF SINES TO TRIANGLES $T_g P_2 C$ AND $T_g P_1 C$:

$$|\overline{D_2 P_2}| = -\rho_g + |\overline{T_g C}|\left[\frac{\sin\left(\frac{\pi}{2} + \frac{\theta_m}{2}\right)}{\sin\left(\frac{\pi}{2} - \frac{\theta_p}{2} - \frac{\theta_m}{2}\right)}\right] = \underline{\underline{8.0708''}},$$

$$|\overline{D_1 P_1}| = -\rho_g + |\overline{T_g C}|\left[\frac{\sin\left(\frac{\pi}{2} - \frac{\theta_m}{2}\right)}{\sin\left(\frac{\pi}{2} + \frac{\theta_m}{2} - \frac{\theta_p}{2}\right)}\right] = \underline{\underline{0.0098''}}.$$

Conclusions

The calculations in the previous sections lead to the following results:

(1) The dipole survey marker coordinates tabulated in Booster Technical Note No. 119 imply dipole alignment target center displacements of 0.0024" for the proximal target, 8.063" for the distal target, measured in the end face planes of the dipole magnet. These calculated displacements do not take into account the effects of a gradual falloff of the dipole fringe magnetic field, and are based on a sharp cutoff fringe field 0.50 gap widths long at each end of the magnet.

(2) Calculations which account for the longer fringing field length and the finite falloff gradient of this field imply that the dipole survey marker points should be offset by 0.007" perpendicular to the line joining their original positions, so that the line joining them is moved inboard (towards the bending center) parallel to itself, by this amount. The line joining the dipole survey marker points remains at precisely 5 degrees to the quadrupole magnetic axis.

The target displacements recommended are 0.010" and 8.071", rather than those calculated for (1).

These are the distances $|\overline{D1\text{-}P1}|$ and $|\overline{D2\text{-}P2}|$, measured in the dipole magnet lamination end planes, of the optical target centers from the dipole survey marker points, required so that the target centers lie on the quadrupole magnetic axis.

(3) The particle trajectory bending radius within the dipole magnet will be 545.837", rather than the value specified in the Booster Design Manual. The dipole magnet current may change, accordingly.

(4) The dipole survey marker positions tabulated in [3] should be adjusted to reflect the additional lateral offset of 0.007" if the target offsets of (2) above are used.

References

[1] H.A. Enge, "Deflecting Magnets", article in A. Septier editor, "Focusing Of Charged Particles , Vol. 2" , Academic Press, N.Y., 1967.

[2] H.A. Enge, Effect of Extended Fringing Fields on Ion-Focusing Properties of Deflecting Magnets, Rev. Sci. Instr. 35, 278 (1964).

[3] G.F. Dell, Coordinates of Magnet Survey Markers and Tunnel Survey Monuments for the AGS Booster. BNL Booster Technical Note No. 119; April 26, 1988.

[4] G. F Dell, Review of Beam Displacement Due To Dipole Fringe Field. Unpublished BNL Note, 10/20/89.

[5] BNL Magnet Measurements Analysis Testing And Measuring Group. TMG-402, August 2, 1989. Test of magnet BMD003.

[6] Booster Design Manual, Revision 1. AGS Booster Project, Accelerator Development Department, Brookhaven National Laboratory, Upton, N.Y., 1988.

APPENDIX 1. COMPUTATION OF THE LENGTH OF A TRAJECTORY CONSISTING OF TWO STRAIGHT SEGMENTS, QS1 AND S2Q' AT FIXED ANGLE θ_m TO ONE ANOTHER, JOINED BY A CIRCULAR ARC OF RADIUS r AND ANGLE θ_m, TANGENT TO BOTH SEGMENTS:

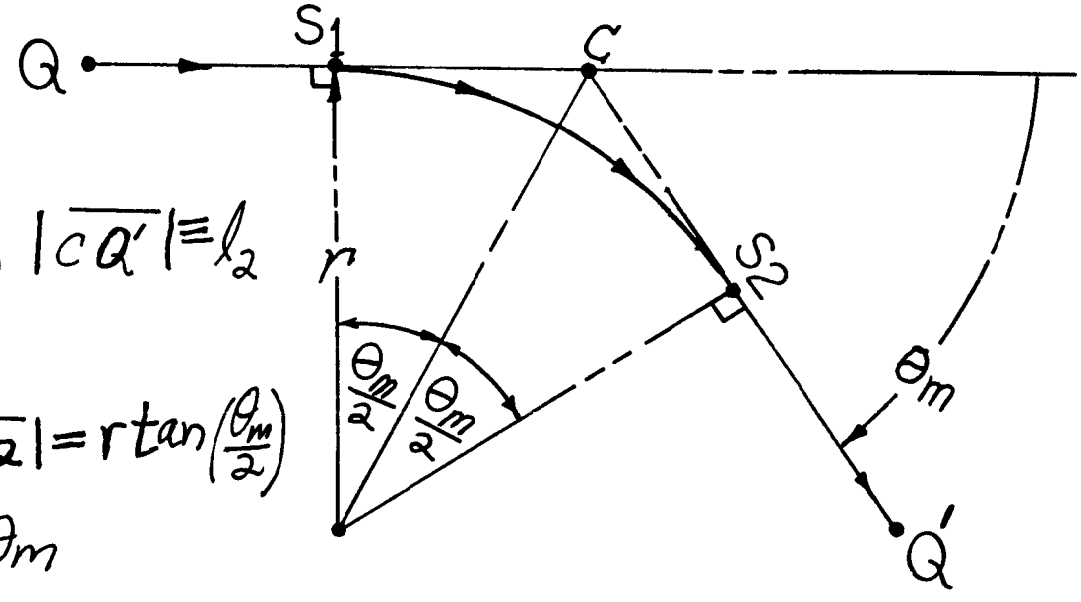

CALL

$$|\overline{QC}| \equiv l_1 \;,\; |\overline{CQ'}| \equiv l_2$$

THEN

$$|\overline{S_1C}| = |\overline{CS_2}| = r\tan\left(\frac{\theta_m}{2}\right)$$

$$\approx |\widehat{S_1S_2}| = r\theta_m$$

$$|\overline{QS_1}| = l_1 - r\tan\left(\frac{\theta_m}{2}\right)$$

$$|\overline{S_2Q'}| = l_2 - r\tan\left(\frac{\theta_m}{2}\right)$$

$$|\widetilde{QQ'}| = |\overline{QS_1}| + |\widehat{S_1S_2}| + |\overline{S_2Q'}|$$

THUS

$$|QQ'| = (l_1 + l_2) + r\left(\theta_m - 2\tan\frac{\theta_m}{2}\right)$$

IF THE BEND RADIUS CHANGES FROM r TO $r+\Delta r$, THE PATH LENGTH CHANGE IS:

$$\Delta|\widetilde{QQ'}| = (\Delta r)\left(\theta_m - 2\tan\frac{\theta_m}{2}\right)$$

FOR $\theta_m = 10°$, $\Delta r = R - \rho_g = 4.457''$,

$$|\Delta\widetilde{QQ'}| = (4.457'')(-0.000444) = \underline{-0.0020''}.$$

FIGURE 5. TRAJECTORY LENGTH CHANGE AS BEND RADIUS CHANGES.

Appendix 2

First Order Computation Of Target Offsets Assuming Short-Tail Fringing Field And Bending Radius Equal To Dipole Magnet Geometric Radius.

The present calculation will demonstrate that the magnetic bending radius must be changed, for particle trajectories through the dipole magnet to be acceptable. The relevant geometry is shown in Fig. 6. The central reference rays used in the optical calculations are the rays SCOFF, SCOFF' which are defined by Enge [1],[2] . These are entry and exit rays which intersect equivalent sharp cutoff fringe field boundary planes at distance R from the bending center. Here R is the magnetic bending radius interior to the magnet. These rays are tangent to the bending circle.

Enge provides ray transfer matrices for the sharp cutoff fringing field (SCOFF) approximation and also for the extended fringing field (EFF) approximation which computes trajectory deviations from the sharp cutoff for known fringe field falloff profiles. The effect of accounting for the extended fringe field profile is to require a lateral shift of the basis rays to generate new basis rays EFF, EFF' laterally offset to SCOFF, SCOFF'. The lateral ray shifts are computed by formulas developed using trajectory perturbation integrals. We will use these results without deriving them here. We restrict our discussion to trajectories lying in the midplane between the pole faces.

As before we let

S1 be the intersection point of SCOFF with VFB,

S2 be the intersection point of SCOFF' with VFB'.

We construct cartesian coordinate systems x_0 , y_0 , z_0 and x, y, z with origins at S1 and S2, respectively, with the y_0-axis perpendicular to SCOFF and y-axis perpendicular to SCOFF'.

We let

S3 be the intersection point of the particle entry ray (along the quadrupole magnetic axis) with the -axis,

d1 be the dipole target center offset distance $|\overline{D1\text{-}P1}|$,

d2 be the dipole target center offset distance $|\overline{D2\text{-}P2}|$.

The angle S1-T-D1 $= \Psi/2$ is very close to $\sin^{-1}\left(\frac{0.62\,g}{\rho_m}\right)$.

FIGURE 6. GEOMETRY FOR FIRST-ORDER RAY OPTICAL CALCULATION OF TARGET OFFSETS, ASSUMING SHORT-TAIL FRINGE FIELD DISTRIBUTION AND BENDING RADIUS EQUAL TO MAGNET GEOMETRIC RADIUS.

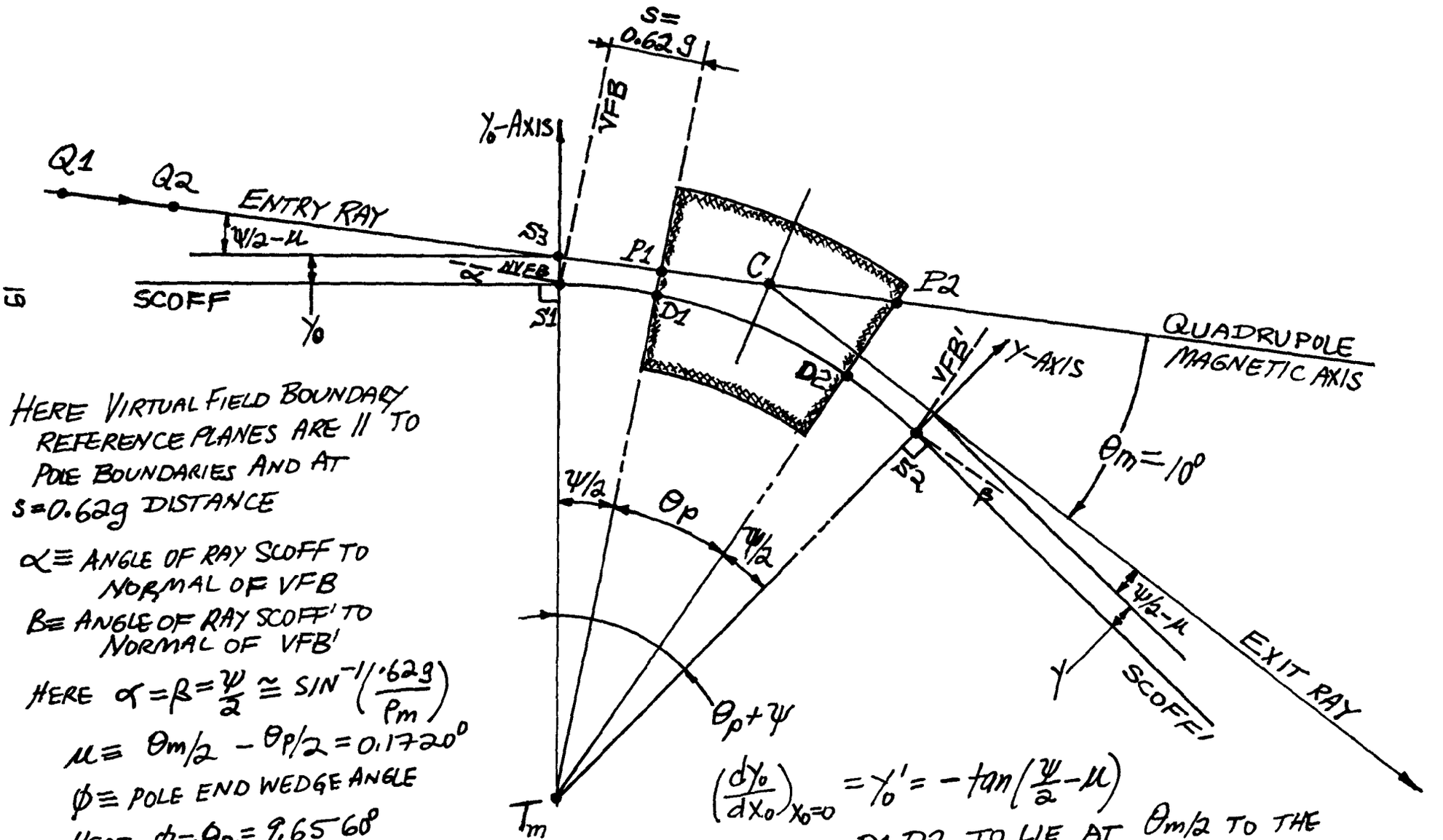

HERE VIRTUAL FIELD BOUNDARY REFERENCE PLANES ARE ∥ TO POLE BOUNDARIES AND AT $s = 0.629$ DISTANCE

$\alpha \equiv$ ANGLE OF RAY SCOFF TO NORMAL OF VFB

$\beta \equiv$ ANGLE OF RAY SCOFF' TO NORMAL OF VFB'

HERE $\alpha = \beta = \frac{\psi}{2} \cong \sin^{-1}\left(\frac{.629}{\rho_m}\right)$

$\mu \equiv \theta_m/2 - \theta_p/2 = 0.1720^0$

$\phi \equiv$ POLE END WEDGE ANGLE

HERE $\phi = \theta_p = 9.6568$

ARC S1-D1-D2-S2 IS A CIRCULAR ARC OF RADIUS

$\rho_m = 541.3776''$

$\left(\frac{dy_0}{dx_0}\right)_{x_0=0} = y_0' = -\tan\left(\frac{\psi}{2} - \mu\right)$

FOR SEGMENT D1 D2 TO LIE AT $\theta_m/2$ TO THE ENTRY RAY WE REQUIRE $\left(\frac{dy}{dx}\right)_{x=0} = y' = -y_0'$.

THE ENTRY RAY OFFSET IS DETERMINED BY THE RAY TRANSFER MATRIX AND THE REQUIREMENT THAT THE ENTRY AND EXIT RAYS EACH ARE AT AN ANGLE $\theta_m/2 = 5°$ TO THE LINE D1 – D2. THIS MEANS THAT FOR

$$\left(\frac{dy_0}{dx_0}\right)_{x_0=0} = y_0' = -\tan\left(\psi/2 - \mu\right) \quad , \text{WHERE} \quad \mu \equiv \theta_m/2 - \theta_p/2 \, , \text{ WE MUST HAVE}$$

$$\left(\frac{dy}{dx}\right)_{x=0} = y' = -y_0' \, .$$

ONCE y_0 IS CALCULATED FROM THE RAY TRANSFER CONDITIONS ABOVE, THE TARGET CENTER OFFSETS $d1, d2$ ARE EASILY FOUND:

FOR TRIANGLE S3-T-P1 WE HAVE $\angle P1\text{-}S3\text{-}T = \frac{\pi}{2} - \left(\frac{\psi}{2} - \mu\right)$, AND BY THE LAW OF SINES

$$\left(\frac{\rho_m + d1}{\rho_m + y_0}\right) = \frac{\sin\left(\frac{\pi}{2} - \left(\frac{\psi}{2} - \mu\right)\right)}{\sin\left(\frac{\pi}{2} - \mu\right)} = \frac{\cos\left(\frac{\psi}{2} - \mu\right)}{\cos\mu} = 1.000042 \quad \text{AND}$$

$$d1 = (\rho_m)\left[1.000042\left(1 + y_0/\rho_m\right) - 1\right] = \underline{0.0023'' + y_0} \, .$$

SIMILARLY $\angle S3\text{-}P2\text{-}T = \frac{\pi}{2} - \theta_p - \mu$, AND THE LAW OF SINES APPLIED TO $\triangle S3\text{-}P2\text{-}T$ GIVES

$$\frac{\rho_m + d2}{\rho_m + y_0} = \frac{\sin\left(\frac{\pi}{2} - \left(\frac{\psi}{2} - \mu\right)\right)}{\sin\left(\frac{\pi}{2} - (\theta_p + \mu)\right)} = \frac{\cos\left(\frac{\psi}{2} - \mu\right)}{\cos(\theta_p + \mu)} = 1.014894$$

AND $$d2 = (\rho_m)\left[1.014894\left(1 + y_0/\rho_m\right) - 1\right] = 8.063'' + y_0 \, .$$

WE NOTE THAT THE TARGET CENTER OFFSETS ARE, CLOSELY, THOSE CALCULATED IN BOOSTER TECHNICAL NOTE NO. 119 PLUS THE ENTRY RAY OFFSET REQUIRED BY THE RAY TRANSFER CONDITION.

FOR A MIDPLANE TRAJECTORY ($z_0 = z_0' = 0$), AND NO SHIFT OF REFERENCE PARTICLE MOMENTUM ($\delta = 0$) THE FIRST ORDER OPTICS IS DESCRIBED BY THE RAY TRANSFER RELATION

$$\begin{pmatrix} y/R \\ y' \end{pmatrix} = \begin{pmatrix} (y/y) & (y/y') \\ (y'/y) & (y'/y') \end{pmatrix} \begin{pmatrix} y_0/R \\ y_0' \end{pmatrix}$$

WHERE $R = \rho_m$ AND THE FIRST ORDER RAY TRANSFER MATRIX IS, FOR THE SHARP CUTOFF FRINGING FIELD APPROXIMATION:

$$\begin{pmatrix} (y/y) & (y/y') \\ (y'/y) & (y'/y') \end{pmatrix} = \begin{pmatrix} \frac{\cos(\phi-\alpha)}{\cos\alpha} & \sin\phi \\ \frac{-\sin(\phi-\alpha-\beta)}{\cos\alpha\cos\beta} & \frac{\cos(\phi-\beta)}{\cos\beta} \end{pmatrix}.$$

HERE ϕ IS THE DIPOLE MAGNET'S WEDGE ANGLE $= \theta_p$.

$\alpha \equiv$ ANGLE OF SCOFF TO THE NORMAL TO VFB.

$\beta \equiv$ ANGLE OF SCOFF' TO THE NORMAL TO VFB'.

IN THE EXTENDED FRINGING FIELD (EFF) MODEL, WE MUST APPLY A CORRECTION TO THE MATRIX ELEMENTS ABOVE, AND REFER DISPLACEMENTS TO THE EFF, EFF' RAYS.

FOR MIDPLANE MOTION THE MATRIX ELEMENTS ARE CORRECTED BY REPLACING α, β BY

$$\alpha_m = \alpha + \Delta\alpha_c$$
$$\beta_m = \beta + \Delta\beta_c$$

FOR SYMMETRIC RAY DIRECTIONS OF $\frac{\text{ENTRY}}{\text{EXIT}}$ RAYS TO $\frac{\text{SCOFF}}{\text{SCOFF'}}$ WE HAVE $\alpha = \beta$, $\Delta\alpha_c = \Delta\beta_c$.

THE CORRECTION ANGLES ARE GIVEN IN REFERENCE [2] BY

$$\Delta\beta_c = -0.6(g/W)^2 f_4(\beta_1) \quad , (46), \text{ FOR A MAGNET WITH FLAT END FACES,}$$

$$\beta_1 = \beta - (1.2\, g/R) I_2 \quad , (43), \text{ WHERE } I_2 = 0.487$$

AND THE FUNCTION $f_4(\beta_1)$ REDUCES TO $f_4(\beta_1) = 0.0096\,(\beta_1/1^\circ)$ FOR SMALL β_1.

SUBSTITUTING $\beta = .213255^\circ$, $\rho_m = R = 1375.099$ cm, $g = 8.255$ cm, $W = 25.4$ cm INTO (46) ABOVE GIVES $\Delta\beta_c = -.000427^\circ$, A SMALL CORRECTION.

USING $\alpha_m = B_m = 0.212828°$ AND $\Phi = 9.6560°$ THE EFF RAY TRANSFER RELATIONS ARE:

$$\begin{pmatrix} Y/R \\ Y' \end{pmatrix} = \begin{pmatrix} .986456 & .167732 \\ -.160406 & .986456 \end{pmatrix} \begin{pmatrix} Y_0/R \\ Y_0' \end{pmatrix} .$$

FOR ENTRY AND EXIT RAYS AT $\theta_m/2 = 5°$ TO CHORD $\overline{D1\text{-}D2}$ WE REQUIRE

$$Y_0' = -Y' = (-1)\tan(\Psi/2 - \mu) = -\tan(.041255°) = -0.00072012 .$$

SET THESE INTO THE EQUATIONS ABOVE TO GET Y_0, THE ENTRY RAY HEIGHT ABOVE EFF AT THE ENTRY PLANE:

$$(+0.00072012) = (-0.160406)(Y_0/541.3776") + (0.986456)(-0.00072012),$$

THUS $Y_0 = -0.7744"$.

THE RAY EFF IS PARALLEL TO SCOFF AND LIES OUTWARD BY $\Delta Y_1 = \frac{0.309\, g^2}{R\cos^2\beta}$, OR $\Delta Y_1 = +0.0060"$. THE ENTRY RAY HEIGHT ABOVE SCOFF IS THEN $Y_0 + \Delta Y_1 = -0.7684"$.

THE FIRST ROW OF THE RAY TRANSFER MATRIX EQUATION GIVES

$$Y/R = .986456\, Y_0/R + 0.167732\, Y_0' \text{ , GIVING}$$

$$Y = -0.8293" \text{ AND } \underline{Y_0 - Y = 0.055"} .$$

THIS MEANS THAT THE EXIT RAY OFFSET IS 0.055" LESS THAN THE ENTRY RAY OFFSET IN THIS CASE, AND THE EXIT TRAJECTORY WOULD NOT BE ON THE OPTIC AXIS OF THE NEXT QUADRUPOLE MAGNET.

THE LARGE AND UNEQUAL RAY OFFSETS REQUIRED PRECLUDE MAGNET OPERATION AT THE BENDING RADIUS SPECIFIED IN THE BOOSTER DESIGN MANUAL. BY OPERATING AT A SOMEWHAT LARGER RADIUS (LOWER MAGNET CURRENT) PROPER OPERATION IS POSSIBLE.